



**Michigan  
Technological  
University**

Michigan Technological University  
**Digital Commons @ Michigan Tech**

---

Dissertations, Master's Theses and Master's Reports

---

2022

## **Per- and Polyfluoroalkyl Substances Mitigation From Contaminated Groundwater Using Halophyte and Cow Bone Biochars**

Bailey Papes

*Michigan Technological University*, [bapapes@mtu.edu](mailto:bapapes@mtu.edu)

Copyright 2022 Bailey Papes

---

### **Recommended Citation**

Papes, Bailey, "Per- and Polyfluoroalkyl Substances Mitigation From Contaminated Groundwater Using Halophyte and Cow Bone Biochars", Open Access Master's Report, Michigan Technological University, 2022.

<https://doi.org/10.37099/mtu.dc.etdr/1362>

Follow this and additional works at: <https://digitalcommons.mtu.edu/etdr>



Part of the [Environmental Engineering Commons](#)

PER- AND POLYFLUOROALKYL SUBSTANCES MITIGATION FROM  
CONTAMINATED GROUNDWATER USING HALOPHYTE AND COW BONE  
BIOCHARS

By

Bailey Papes

A REPORT

Submitted in partial fulfillment of the requirements for the degree of

MASTER OF SCIENCE

In Environmental Engineering

MICHIGAN TECHNOLOGICAL UNIVERSITY

2022

© 2022 Bailey Papes

This report has been approved in partial fulfillment of the requirements for the Degree of  
MASTER OF SCIENCE in Environmental Engineering.

Department of Civil, Environmental and Geospatial Engineering

Report Advisor: *Dr. Jennifer Becker*

Committee Member: *Dr. Eric Seagren*

Committee Member: *Dr. David Watkins*

Department Chair: *Dr. Audra Morse*

# Table of Contents

List of Figures .....	iv
List of Tables .....	v
Acknowledgements .....	vii
List of Abbreviations .....	viii
Abstract .....	ix
1 Introduction.....	1
1.1 Per and Polyfluoroalkyl Substances .....	1
1.2 Biochar .....	3
2 Goal and Objectives .....	6
3 Materials and Methods.....	7
3.1 Site Description .....	7
3.2 Water .....	9
3.3 Adsorbents.....	9
3.3.1 Halophyte Biochar BGNDRF .....	9
3.3.2 Halophyte Biochar NMSU.....	10
3.3.3 Bone Char .....	10
3.3.4 Powdered Activated Carbon (PAC).....	10
3.4 Slurry Solutions .....	10
3.5 Batch Testing.....	11
3.6 Analytical methods.....	11
4 Results and Discussion .....	13
4.1 Adsorbent Characteristics: Specific Surface Area and Elemental Analysis ..	13
4.2 Adsorption of PFAS to Biochar .....	14
4.3 Impacts of adsorbents on DOM and aqueous inorganic ions concentrations.	18
5 Summary and Future Work.....	23
6 Reference List .....	24
A Appendix.....	23

## List of Figures

<b>Figure 3-1:</b> Map of New Mexico indicating the location of BGNDRF in Alamogordo, NM .....	7
<b>Figure 3-2:</b> Map of Alamogordo's proximity to the Holloman Air Force Base (Left) and map of the four wells' location at BGNDRF (Right) (Newton & Land, 2016).....	8
<b>Figure 3-3:</b> Jar test apparatus .....	11
<b>Figure 4-1:</b> Normalized concentrations of (a) PFHxS, (b) PFOS, and (c) PFOA as a function of adsorbent doses from 0-1000 mg/L. Error bars indicate $\pm 1$ standard deviation of duplicate measurements.....	16
<b>Figure 4-2:</b> Concentration ( $C_e$ ) of (a) PFOA, (b) PFOS, and (c) PFHxS after two hours versus the adsorption capacity at equilibrium ( $q_e$ ) for halophyte biochar BGNDRF. ....	17
<b>Figure 4-3:</b> (a) Normalized DOC concentration and (b) normalized $A_{254}$ , as a function of adsorbent dose. Error bars indicate standard deviation of duplicate jars, where $C$ represents final concentration, $C_0$ represents the initial concentration, $A$ represents final absorbance, and $A_0$ represents initial absorbance. Symbols represent the average of the replicate jars. Error bars represent $\pm 1$ standard deviations of duplicate measurements. In panel (a), the dashed horizontal line represents the method detection limit (0.0616 mg/L). ....	21

## List of Tables

<b>Table 1-1:</b> Physical and chemical properties of PFOA, PFOS, and PFHxS .....	2
<b>Table 1-3:</b> Summary of feedstocks, biochar concentrations and properties, and PFAS adsorbates used in reported PFAS-biochar adsorption studies. ....	5
<b>Table 3-1:</b> PFAS concentrations measured in BGNDRF wells in February 2019 (NMED, 2019) .....	8
<b>Table 3-2:</b> Average historical data collected twice yearly for well 2 groundwater from June 2015 to November 2020 (BGNDRF, 2022) .....	9
<b>Table 4-1:</b> Adsorbent specific surface area for PAC and biochars .....	13
<b>Table 4-2:</b> Elemental concentrations of PAC and biochars reported in PFAS sorption studies .....	14
<b>Table 4-3:</b> Maximum sorption capacity of biochars and PAC for PFOA, PFOS, and PFHxS reported in adsorption studies.....	18
<b>Table 4-4:</b> Chemical and physical properties of untreated groundwater obtained from Well 2.....	18
Table A-1: PAC jar test alkalinity, pH, temperature, A <sub>254</sub> , and conductivity for doses of 10, 50 and 100 mg/L .....	23
Table A-2: Halophyte (BGNDRF) jar test alkalinity, pH, temperature, A <sub>254</sub> , and conductivity for doses of 10, 50 and 100 mg/L .....	24
Table A-3: Halophyte (NMSU) jar test alkalinity, pH, temperature, A <sub>254</sub> , and conductivity for doses of 10, 50 and 100 mg/L .....	24
Table A-4: Bone char jar test alkalinity, pH, temperature, A <sub>254</sub> , and conductivity for doses of 10, 50 and 100 mg/L.....	25
Table A-5: Halophyte (BGNDRF) jar test alkalinity, pH, temperature, A <sub>254</sub> , and conductivity for doses of 200, 500 and 1000 mg/L .....	26
Table A-6: Halophyte (NMSU) jar test alkalinity, pH, temperature, A <sub>254</sub> , and conductivity for dose of 200, 500 and 1000 mg/L.....	26
Table A-7: Bone char jar test alkalinity, pH, temperature, A <sub>254</sub> , and conductivity for doses of 200, 500 and 1000 mg/L.....	27
Table A-8: Nitrate absorbance for PAC, Halophyte (BGNDRF) and Halophyte (NMSU) biochar.....	27
Table A-9: Nitrate absorbance for bone char.....	28
Table A-10: DOC concentrations, average, standard deviation, normalized concentration, and removal for adsorbent doses 10, 50 and 100 mg/L .....	29
Table A-11: DOC concentrations, average, standard deviation, normalized concentration, and removal for adsorbent doses 200, 500 and 1000 mg/L .....	30

Table A-12: PFAS average concentrations, normalized concentrations and removal for doses of 10, 50 and 100 mg/L.....	31
Table A-13: PFAS average concentrations, normalized concentrations and removal for doses of 200, 500 and 1000 mg/L.....	32
Table A-14: PFAS concentration data, average concentration, and standard deviations for doses 10, 50 and 100 mg/L .....	33
Table A-15: PFAS concentration data, average concentration, and standard deviations for doses 200, 500 and 1000 mg/L .....	34
Table A-16: PFOA, PFOS, and PFHxS adsorption capacity at equilibrium .....	35

## **Acknowledgements**

I would like to thank the Bureau of Reclamation's Brackish Groundwater National Desalination Research Facility staff for all their assistance while I conducted this research. I wish to show my appreciation to Dr. Anthony Kennedy for being my mentor and giving me valuable guidance and technical support throughout my internship. Additionally, thank you to my advisor, Dr. Jennifer Becker, and my committee members, Dr. Eric Seagren and Dr. David Watkins for their feedback and help with completing this report.



## List of Abbreviations

BGNDRF	Brackish Groundwater National Desalination Research Facility
DI	Deionized water
DOC	Dissolved organic carbon
EPA	Environmental Protection Agency
GAC	Granular activated carbon
HDPE	High density polyethylene
MCL	Maximum contaminant level
NMSU	New Mexico State University
PAC	Powder activated carbon
PFAS	Per- and polyfluoroalkyl substances
PFCA	Perfluoroalkyl carboxylic acids
PFHxS	Perfluorohexane sulfonic acid
PFOA	Perfluorooctanoic acid
PFOS	Perfluorooctane sulfonic acid
PFSA	Perfluoroalkyl sulfonic acids
pH <sub>pzc</sub>	pH at the point of zero charge
q <sub>max</sub>	Maximum sorption capacity
RO	Reverse osmosis
TDS	Total dissolved solids
A <sub>254</sub>	Ultraviolet absorbance at 254 nm

## **Abstract**

Per and polyfluoroalkyl substances (PFAS) groundwater contamination is a growing concern for the Brackish Groundwater National Desalination Research Facility. Two of the four wells onsite are contaminated with perfluorooctanoic acid (PFOA), perfluorooctane sulfonic acid (PFOS) and perfluorohexane sulfonic acid (PFHxS). The removal of PFAS by adsorption onto powder activated carbon (PAC) is promising, but production of PAC is energy intensive and expensive. A potential cost-effective alternative to PAC is biochar. This study quantified the capacities of two halophyte biochars, cow bone biochar and PAC to adsorb PFOA, PFOS, and PFHxS from brackish groundwater. The three biochars were ineffective at adsorbing the PFAS compounds at low adsorbent doses (10-100 mg/L) because of their low surface area. Increasing the biochar adsorbent dose to 200, 500 and 1000 mg/L allowed for comparable PFAS absorption by one of the halophyte biochars.

# 1 Introduction

## 1.1 Per and Polyfluoroalkyl Substances

An emerging class of contaminants that have gained public and academic attention in recent years is per- and polyfluoroalkyl substances (PFAS). Due to PFAS' omniphobic properties, they are found in a wide variety of commercial products, including non-stick cookware, adhesives, fast food packaging, waterproof clothing, and fire-fighting foam (Sun et al., 2016). The past 60 years of industrial use and disposal of PFAS have resulted in the substances being detected in environmental waters, soil, and air. PFAS can be found even in very remote places like Antarctica and in the blood of entire populations in developed countries (Del Vento, 2012, Fenton, 2020).




The chemical structure of PFAS consists of a carbon chain with a minimum of one fully fluorinated carbon and a charged functional group, typically a carboxylic acid or sulfonic acid, at the end (Teaf et al., 2019). PFAS can be classified by their functional group into perfluoroalkyl carboxylic acids (PFCA) and perfluoroalkyl sulfonic acids (PFSA), and into long and short carbon chain compounds. PFCA consisting of eight or more carbons and PFSA composed of six or more carbons are classified as long chain compounds, while PFCA with seven or less carbons and PFSA with five or less carbons are classified as short chain compounds (OECD, 2018). PFAS have both hydrophobic and lipophobic properties (Gagliano et al., 2020). The bond between carbon and fluorine has high thermal and chemical stability, which make these compounds resistant to photolysis, hydrolysis, biodegradation, and metabolic processes in nature (Teaf et al., 2019, Wanninayake, 2021). PFAS have lengthy biological half-lives ranging from 2.3 to 5.4 years and are known to bioaccumulate within the environment and animals (Gagliano et al., 2020). The bioaccumulation of PFAS is of concern because the specific toxicity of these compounds is still largely unknown. However, exposure to PFAS has been linked to reduced antibody production from vaccines, thyroid disease, reproductive issues, liver problems and kidney and testicular cancer (Fenton, 2020).

There are 4730 PFAS that have been documented and assigned CAS numbers (OECD, 2018). Some of the most widely studied PFAS are perfluorooctanoic acid (PFOA), perfluorooctane sulfonic acid (PFOS) and perfluorohexane sulfonic acid (PFHxS). Manufacturers in the United States have phased out PFOA and PFOS from production because of increased public awareness of their potential health effects, the prospects of lawsuits, and regulatory pressure (Pontius, 2019). However, humans can still be exposed to PFOA and PFOS from legacy uses, imported goods from countries that still produce PFOA and PFOS, and PFOA and PFOS in the environment (Pontius, 2019).

Key physical and chemical properties of PFOA, PFOS and PFHxS are summarized in Table 1-1. PFOA, PFOS, and PFHxS are long chain compounds and are presented as anionic compounds in water due to their low  $pK_a$  values. The functional end groups impact the adsorption properties of PFAS. When comparing compounds of the same carbon chain length, PFSA are more hydrophobic and more easily adsorbed than PFCA (Du et al, 2014, Gagliano et al., 2020). As the carbon chain length increases for

substances with the same end functional group, water solubility decreases, and the substances are more hydrophobic (Du et al., 2014). For example, PFHxS and PFOS share the same sulfonic functional group, but PFHxS has two fewer carbons and is more soluble in water than PFOS.

**Table 1-1:**Physical and chemical properties of PFOA, PFOS, and PFHxS

	Perfluorooctanoic acid (PFOA)	Perfluorooctane Sulfonic Acid (PFOS)	Perfluorohexane Sulfonic Acid (PFHxS)	Units
Formula	C <sub>8</sub> HF <sub>15</sub> O <sub>2</sub>	C <sub>8</sub> HF <sub>17</sub> O <sub>3</sub> S	C <sub>6</sub> HF <sub>13</sub> O <sub>3</sub> S	
Structure				
MW	414.07	500.13	400.12	g/mol
pKa	0.5	-3.27	-3.34	
Solubility <sup>1</sup> in water	13	7.5	150	g/L
Log D <sup>1</sup>	2.69	1.01	-0.45	

<sup>1</sup> Property at 25 °C and pH of 8

Source: SciFinder, 2021

Treatment of water to remove and destroy PFAS is challenging because of the strength of the carbon-fluorine bond. Conventional drinking water treatment processes such as coagulation, flocculation, sedimentation, filtration, and disinfection with free chlorine are ineffective at removing and destroying PFAS (Hopkins et al, 2018). PFAS adsorption onto powdered and granular activated carbon (PAC and GAC, respectively) is promising for the removal of aqueous PFAS (Zhang et al., 2019, Galiano et al., 2020, Du et al., 2014). However, production of PAC and GAC is expensive and has large energy demands because of the high temperatures and the activation processes that are required (Tan et al., 2015). Several recent studies evaluated the use of biochar as a cost-effective, less energy-intensive, and sustainable adsorbent that could be used in lieu of PAC for adsorbing aqueous PFAS (Tan et al., 2015, Wanninayake, 2021). Sorption of PFAS to biochar is also the focus of the current study.

The predominant mechanisms for the adsorption of PFAS onto several adsorbent materials (PAC, some biochars) are electrostatic and hydrophobic interactions (Gagliano et al., 2020). The solution pH, properties of adsorbate (PFOA, PFOS) and initial concentrations, characteristics of the adsorbent, and co-existing anions and cations including dissolved organic matter (DOM) can impact the adsorption capabilities of biochar (Wanninayake, 2021, Du et al., 2014).

## 1.2 Biochar

Biochar is a carbonaceous substance that is produced by heating biomass in the absence of oxygen (Tan et al., 2015). A wide variety of biomass feedstock materials can be used to generate biochar, including wood, agricultural waste, wastewater biosolids, and animal bones (Dai et al., 2019). Most biochar feedstocks occur in abundance, are typically considered waste products, and sequester carbon, all of which, makes biochar an extremely sustainable adsorbent. Research has focused on the use of biochar as an adsorbent in aqueous solutions for the removal of organic and non-organic pollutants.

One potential feedstock material is halophytes, which are salt-tolerant plants. Halophytes can be irrigated by using reverse osmosis (RO) concentrate, which contains elevated concentrations of ions, and is produced during the treatment of brackish groundwater and seawater. Another potential feedstock material is cow bones, which are a waste product of animal agriculture and meat processing operations.

Physical and chemical properties of biochar are dependent on the feedstock, residence time, and pyrolysis temperature (Cantrell et al., 2012). Biochar is produced at pyrolysis temperatures ranging from 200 °C to 900 °C and with residence times from a few seconds to days (Ahmad et al., 2014). As the pyrolysis temperature increases so does the surface area of biochar, likely because of the decomposition of organic matter, formation of micropores, and destruction of aliphatic alkyls and ester groups which exposes the aromatic lignin core (Cantrell et al., 2012). Pyrolysis also rearranges and breaks the chemical bonds of the surface functional groups on biochar to produce oxygenated hydrocarbons (carboxyl, hydroxyl, phenolic etc.) (Cantrell et al., 2012, Ahmad et al., 2014). At high pyrolysis temperatures, biochar appears to have organized carbon layers and fewer surface functional groups (Cantrell et al., 2012). Biochars produced at higher pyrolysis temperatures have larger surface areas which has been shown to increase biochar adsorption capabilities for PFAS in aqueous solutions (Kundu et al., 2021, Guo et al., 2017).

An increasing number of research studies have been conducted to characterize the capacities and kinetics of biochars for the removal of PFAS from aqueous solutions. The motivation for biochar adsorption studies, especially for the removal of PFAS, is the hope that a cost effective and sustainable adsorbent will be identified with a high affinity for PFAS. Most studies have used GAC-sized particles (0.2 to 5 mm) and included adsorption kinetic assays, isotherms, and assessment of the impacts of pH on adsorption performance (Deng et al., 2015, Guo et al., 2017, Inyang & Dickenson, 2017, Kundu et al., 2021, Seigerwald & Ray, 2021, Zhang et al., 2021). PFOS and PFOA adsorption from synthetic waters have been most widely studied, but increasingly, research on the adsorption of shorter chain PFAS and adsorption from wastewater and lake water are being investigated (Kundu et al., 2021, Inyang & Dickenson, 2017).

Key biochar properties and the experimental conditions used in recent studies of the adsorption of PFAS to biochar are summarized in Table 1-2. The adsorbent (biochar) dosage varied from 50 to 20,000 mg/L. The adsorbent surface area is measured in most

studies to investigate the adsorption capacities, but research has shown that adsorbent surface area alone may not be the best indicator of adsorption capabilities and more attention is being shown to the adsorbent's pH at zero-point charge,  $\text{pH}_{\text{zpc}}$  (Guo et al., 2017, Inyang & Dickenson, 2017, Seigerwald & Ray, 2021). The  $\text{pH}_{\text{zpc}}$  indicates the surface charge of the adsorbent at the experimental pH and determines the adsorption mechanism between PFAS and the adsorbent.

**Table 1-2:** Summary of feedstocks, biochar concentrations and properties, and PFAS adsorbates used in reported PFAS-biochar adsorption studies.

Biochar	Dosage (mg/L)	PFAS	Specific Surface Area  (m <sup>2</sup> /g)	pH <sub>zpc</sub>	Source
Softwood	50	PFOS PFOA PFBS PFBA	459	6.1	Zhang et al. (2021)
Peach pit	333	PFBA,	6.4	6.1	Inyang & Dickenson (2017)
Spruce pine wood		PFPnA	98.8	10.3	
Wood-mixed poultry litter		PFHxA	14.8	6.4	
Pinewood		PFHxS	413	9.2	
Hardwood		PFHpA PFOA PFOS PFNA PFDA	453	7.0	
Sawdust	20,000	PFOS	79.87	-	Kundu et al. (2021)
Biosolids		PFOA	55.29	-	
		PFHxS			
		PFBS			
		PFPeS			
		PFHpS			
		PFDoA PFTTrDA			
Bamboo derived GAC activated with KOH	100	PFOS PFOA	2,450	-	Deng et al. (2015)
Spent coffee grounds activated with KOH	100	PFOS	858	-	Steigerwald & Ray (2021)
Mountain Crest Gardens biochar (wood-based)			801		
Corn-straw derived biochar	200	PFOS			Guo et al. (2017)
BC250			2.5	-	
BC400			3.75	-	
BC550			41.10	-	
BC700			297.58	10.3	

## **2 Goal and Objectives**

The goal of this study was to conduct proof-of-concept experiments to evaluate the feasibility of using biochar to remove three PFAS compounds (PFOA, PFOS, and PFHxS) from contaminated brackish groundwater. The specific objectives of this study were to:

1. Create halophyte biochar using two different techniques and temperatures, and
2. Simulate PFAS removal by PAC addition in drinking water treatment trains by using a jar test experiment operated for two hours, and
3. Compare the adsorption capacities of halophyte and cow bone biochars to a commercial PAC while investigating the impacts of DOM and inorganic ion concentrations on PFAS adsorption.

This research expands on current biochar adsorption literature by using brackish groundwater, which could also be representative of some reverse osmosis concentrates (e.g., from wastewater reuse), and PAC-sized particles. In contrast, most studies focusing on PFAS adsorption have used synthetic waters or deionized (DI) water and GAC-sized particles (Gagliano et al., 2020). Additionally, halophyte and cow bone biochars have not been utilized for PFAS adsorption studies to date.



### 3 Materials and Methods

#### 3.1 Site Description

The Bureau of Reclamation's Brackish Groundwater National Desalination Research Facility (BGNDRF) is located in Alamogordo, NM (Figure 1-1). BGNDRF focuses on pilot scale testing of new and innovative water treatment processes for the desalination of brackish and impaired groundwater. Onsite, there are four wells that produce water containing total dissolved solid (TDS) concentrations ranging from 1,000 to 5,000 mg/L. The brackish water is provided to clients to meet their experimental needs.



**Figure 3-1:** Map of New Mexico indicating the location of BGNDRF in Alamogordo, NM

In February 2019, water samples from all four wells onsite were collected by the New Mexico Environmental Department for PFAS analysis, due to the wells' proximity to the Holloman Air Force Base, which is known to do extensive training using firefighting foam containing PFAS (NMED, 2021). The results of the initial tests are shown in Table 3-1 and indicate that PFAS is present in Well 2 and 4 (Figure 3-2) (NMED, 2019). There are currently no national Maximum Contaminant Levels (MCLs) for any PFAS compounds, but the Environmental Protection Agency (EPA) has issued a health advisory level (HAL) of 70 parts per trillion (ppt) for the sum of PFOA and PFOS concentrations in drinking water (USEPA, 2020). HALs are non-regulatory and non-enforceable. Currently, the concentration in both wells is greater than the HAL. The EPA

does not have a set standard for PFAS concentrations for wastewater discharges. Several individual cities and states have established PFAS drinking water and discharge requirements that are stricter than the EPA's HAL. After the results from the analyses of the groundwater at BGNDRF were published, the city of Alamogordo required BGNDRF to have non-detectable levels of all PFAS in water discharged to the city's wastewater treatment facility. The city of Alamogordo uses reclaimed wastewater to water the community's parks and golf course and wanted to ensure that PFAS was not further spread throughout the community. This has caused numerous challenges for the disposal of water from BGNDRF.

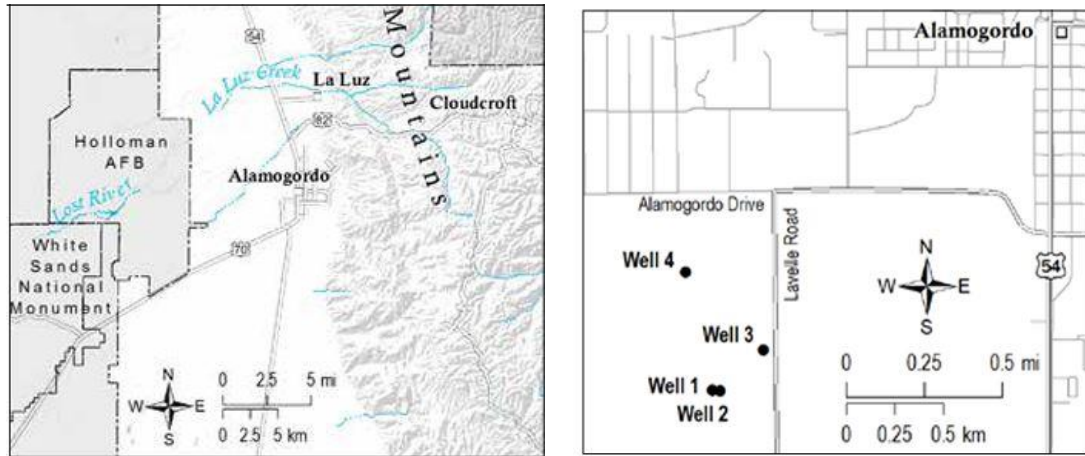


**Figure 3-2:** Map of Alamogordo's proximity to the Holloman Air Force Base (Left) and map of the four wells' location at BGNDRF (Right) (Newton & Land, 2016)

**Table 3-1:** PFAS concentrations measured in BGNDRF wells in February 2019 (NMED, 2019)

Well	Concentration (ng/L)			
	1	2	3	4
<b>PFHxS</b>	ND <sup>a</sup>	9.6	ND	5.3
<b>PFOA</b>	ND	220	ND	120
<b>PFOS</b>	ND	16	ND	24
<b>PFBA</b>	ND	11	ND	3.5
<b>PFBS</b>	ND	4.9	ND	ND
<b>PFPeA</b>	ND	5.4	ND	ND
<b>PFHxA</b>	ND	6.3	ND	2.3
<b>PFHpA</b>	ND	5.8	ND	2.4
<b>Total PFAS<sup>b</sup></b>	0	279	0	159
<b>Total PFOA + PFOS</b>	0	236	0	144

<sup>a</sup>ND = Not detected.

<sup>b</sup>A Total of 21 PFAS were analyzed, and all other substances were ND.

Groundwater from Well 2 was selected for use in this experiment, because the TDS and PFAS concentrations are higher in the Well 2 water compared with the Well 4 water. Well 2 obtains water from the basin fill aquifer in the Tularosa Basin, which supplies water for most of the population in the area (Newton & Land, 2016). Well 2 was drilled on November 11, 2003, has a total depth of 248 feet, and yields water with a TDS concentration of approximately 5,000 mg/L (Malcolm Pirnie, Inc., 2003). Table 3-2 provides a summary of the average chemical properties of Well 2 groundwater collected from June 2015 to November 2020 twice each year.

**Table 3-2:** Average historical data collected twice yearly for well 2 groundwater from June 2015 to November 2020 (BGNDRF, 2022)

Parameter	Value <sup>a</sup>	Units
TDS (Total Dissolved Solids)	5,322 ± 625	mg/L
Calcium (Ca <sup>2+</sup> )	480 ± 19	mg/L
Chloride (Cl <sup>-</sup> )	570 ± 59	mg/L
Magnesium (Mg <sup>2+</sup> )	311 ± 24	mg/L
Sodium (Na <sup>+</sup> )	638 ± 123	mg/L
Sulfate (SO <sub>4</sub> <sup>2-</sup> )	2,811 ± 530	mg/L
Nitrate (NO <sub>3</sub> <sup>-</sup> )	7.2 ± 1.5	mg N/L
Potassium (K <sup>+</sup> )	2.4 ± 0.3	mg/L
Alkalinity	223 ± 26	mg/L as CaCO <sub>3</sub>
pH	7.4 ± 0.3	

<sup>a</sup>Average ± 1 standard deviation (n =12)

## 3.2 Water

The brackish groundwater used in this study was collected from Well 2 at BGNDRF on June 11, 2021 and was stored indoors at room temperature in a 1000-L, high density polyethylene (HDPE) tote for the duration of all experiments.

## 3.3 Adsorbents

### 3.3.1 Halophyte Biochar BGNDRF

Halophyte biochar BGNDRF was created using the halophyte species *Atriplex lentiformis*. *A. lentiformis* was grown at BGNDRF and watered by drip irrigation using a combination of brackish groundwater and RO concentrate (Cerra, Shukla, & O'Meara, 2021). Two *A. lentiformis* plants were harvested using a cordless electric pole saw, and the branches were cut into approximately 3-cm pellets using garden shears. Leaves were not included in the biochar production protocol. Branch pellets were then dried in an oven (Gravity Convection Incubator Model 17, Precision Scientific Thelco, Illinois) for 24 hours at 100 °C to remove excess moisture. Dried pellets were then packed into three separate alumina crucibles (Thomas Scientific, New Jersey) with lids to limit oxygen intrusion and placed inside a muffle furnace (Lindberg/ Blue Moldatherm 1100 °C Box

Furnace, ThermoFisher Scientific, Massachusetts). Crucibles and biochar were then heated to 700 °C over 6 hours and 45 minutes to ensure that the crucibles did not heat up faster than 150 °C per hour to prevent cracking (XTech Lab Supplies, 2022). The muffle furnace was then held at 700 °C for one hour and cooled to room temperature (25 °C) for approximately 15 hours. After cooling, biochar was removed and crushed into a fine powder for jar testing. PAC-type particle sizes were obtained by manually grinding using a mortar and pestle and sieving to less than US standard mesh size 200 (particle diameter of 75 µm) using a vibratory sieve shaker (Vibra Pad SS-28, Gilson Company Inc., Ohio). This biochar is designated herein as halophyte biochar BGNDRF.

### **3.3.2 Halophyte Biochar NMSU**

Halophyte Biochar NMSU was created from the *A. lentiformis* dried pellet stock used to produce halophyte biochar BGNDRF. The pellets were further processed by New Mexico State University (NMSU, Las Cruces, NM), as described below. for alternative biochar production. At NMSU, pellets were ground in a mill (Cutting Mill SM 300, Retsch GmbH, Germany) fitted with a 2-mm trapezoidal screen. Pellets were then packed in a custom built pyrolyzer (Zhang, Idowu, & Brewer, 2016, Amidei, 2021) and heated to 600 °C for 1 hour under nitrogen gas (N<sub>2</sub>) flow to limit oxygen intrusion. The biochar was further processed into PAC-type particle size following the same procedure as the halophyte biochar BGNDRF. This biochar is designated herein as halophyte biochar NMSU.

### **3.3.3 Bone Char**

Cow bone biochar was obtained from a commercial supplier (Confluence Energy, Kremmling, Colorado) as approximately 3-cm granules. Specific pyrolysis conditions were not provided because it is a proprietary product, but the cattle bones were processed by packing them into a biochar retort and pyrolyzed for approximately 8 hours at temperatures ranges from 350 °C to 650 °C (Kennedy, & Arias-Paic, 2020). Cow bone granules were processed following the same procedure as the halophyte biochars. This biochar is designated herein as bone char.

### **3.3.4 Powdered Activated Carbon (PAC)**

A commercial PAC (WPH-M) was obtained from Calgon Carbon (Pennsylvania) WPH-M PAC had 95% of the particles passing mesh size 200. Consequently, no further processing of the PAC was required prior to jar testing.

## **3.4 Slurry Solutions**

The biochars and PAC described above were added to RO water (conductivity <70 µS/cm) at a concentration of 20 g/L. The solutions were prepared using volumetric flasks and were stirred on high using a magnetic stir plate and bar for 30 minutes. Slurry solutions were transferred to 500-mL amber glass bottles with no headspace for storage and placed in a cabinet with glass doors at room temperature (25 °C). Slurry solutions were stirred again in 500-mL glass beakers before use in jar testing.

### 3.5 Batch Testing

Before each batch test, the untreated groundwater pH, alkalinity, temperature, conductivity, and ultraviolet absorbance at 254 nm ( $A_{254}$ ) were measured according to the methods described below. Samples of untreated groundwater were also collected for analysis of PFAS and DOC by external laboratories. For all experiments, a six-jar programmable jar tester (PB-900, Phipps & Bird, Inc., Virginia) was used. Each of the six jars were filled with 2.0 L of Well 2 groundwater, as shown in Figure 3-1. Duplicate jars were dosed with adsorbents at 10, 50, or 100 mg/L. Plastic syringes were filled with a continuously stirred adsorbent solution and used to spike the jars during an initial rapid mix phase (1 min, 300 RPM). The jars were then mixed for 2 hours at 60 RPM. These mixing regimes were repeated for all adsorbents. At the end of 2 hours mixing period, treated groundwater was filtered through 45  $\mu$ m filters (Nylon Membrane Filter, Cole-Parmer, Illinois) using a filter holder and peristaltic pump connected to a pressure gauge. The filtrate was analyzed for DOC, by measuring dissolved organic carbon (DOC) concentration, and  $A_{254}$ . The filtrate was also analyzed for PFOA, PFOS, and PFHxS concentrations. Unfiltered water was analyzed for final pH, temperature, and conductivity. After results of the initial jar tests were obtained, the jar test experiments were repeated for all biochars, at doses of 200, 500, and 1,000 mg/L.



**Figure 3-3:** Jar test apparatus

### 3.6 Analytical methods

A portable benchtop multimeter (PC 700 Oakton, Illinois) with a gel-filled electrode (59001-65; Oakton) and epoxy/platinum electrode (WD-35608-78; Oakton) were used to measure the pH and both the conductivity and temperature, respectively. A digital titrator with sulfuric acid was used to measure untreated groundwater alkalinity following Hach Method 8023 (Hach, Colorado).  $A_{254}$  was measured according to Standard Method 5910 (APHA et al. 2017) using a spectrophotometer (DR 6000, Hach, Colorado). Nitrate concentrations in duplicate groundwater samples treated with 100 mg/L of each adsorbent was measured spectrophotometrically (Method 8171, Hach, Colorado). DOC was measured in duplicate by an external, certified laboratory (Green Analytical

Laboratories, Colorado) according to Standard Method 5310C using a TOC analyzer (TOC V-WP, Shimadzu, Japan). PFAS concentrations were measured by an external, certified laboratory (ASL Environmental, Washington) using liquid chromatography–mass spectrometry according to method PFC/537M. Samples of each adsorbent were transferred to NMSU for nitrogen gas adsorption analysis using a sorption analyzer (ASAP 2050, Micromeritics, Georgia). Additionally, NMSU measured the inorganic elemental composition of the adsorbents using an inductively coupled plasma analyzer (Optima 4300 DV ICP-OES, Perkin Elmer, Massachusetts).

## 4 Results and Discussion

### 4.1 Adsorbent Characteristics: specific surface area and elemental composition

PFAS removal from aqueous solution is influenced by the adsorbent's specific surface area and elemental composition. The specific surface areas of the adsorbents are shown in Table 4-1. PAC had approximately 10 to 100 times more surface area than the biochars, which explains why it exhibited better adsorption capacities for PFAS. The surface areas of PAC and bone char measured in the current study are consistent with published values (Li et al., 2003; Kennedy & Arias-Paic, 2020). Of the halophyte biochars, BGNDRF had more surface area than NMSU, presumably because a higher pyrolysis temperature was used during production of halophyte biochar BGNDRF compared to that used for halophyte biochar NMSU. Surface area alone is not the best predictor of adsorption capabilities, and other research has suggested using an adsorbent's  $\text{pH}_{\text{pzc}}$  to help predict its adsorption capabilities (Steigerwald & Ray, 2021). Unfortunately,  $\text{pH}_{\text{pzc}}$  values were not measured in this study.

**Table 4-1:** Adsorbent specific surface area for PAC and biochars

Adsorbent	Total Specific Surface Area ( $\text{m}^2/\text{g}$ )
PAC	941
Halophyte biochar BGNDRF	73
Halophyte biochar NMSU	1.8
Bone Char	90

The elemental analysis results are shown in Table 4-2. The halophyte biochar NMSU contained lower concentrations of all elements compared to halophyte biochar BGNDRF. Other studies analyzing the impact of pyrolysis temperature on biochar elemental composition showed similar results (Fidel et al., 2017, Wei et al., 2019). As the pyrolysis temperature increased, more organic matter decomposition occurred with higher levels of carbonization resulting in higher concentrations of alkaline elements. The elements at the highest concentrations in the halophyte biochars were potassium, sodium, and calcium. This was not surprising because the halophytes were grown with RO concentrate containing high levels of calcium, potassium, sodium and magnesium, and the ions were shown to be taken up by the plants (Cerra, Shukla, & O'Meara, 2021). The bone char has high levels of calcium and phosphorus. PAC contained the lowest concentrations of inorganic elements.

**Table 4-2:** Elemental concentrations of PAC and biochars reported in PFAS sorption studies

Element concentration (mg/kg adsorbent)	PAC	Halophyte biochar BGNDRF	Halophyte biochar (NMSU)	Bone Char
Fe	4,664	518	201	381
Mn	18	60	40	19
Ca	2,062	17,800	11,160	305,000
Mg	387	9,615	6,117	6,037
P	199	904	611	131,600
K	547	19,590	16,960	3,875
Na	1,180	18,220	13,680	9,181
S	525	1,769	1,302	1,045

## 4.2 Adsorption of PFAS to Biochar

Full scale drinking water treatment for the adsorption of PFAS onto PAC and biochars was simulated using jar test experiments. In a typical drinking water treatment train, PAC is added to the source water upstream of other treatment processes. The PAC addition is followed by rapid mix and flocculation treatment processes (AWWA, 2020). The typical mean velocity gradient ( $G$ ) for rapid mix ranges from 500 - 6000  $s^{-1}$ , while the mean velocity gradient for flocculation ranges from 50 – 100  $s^{-1}$  (Metcalf & Eddy, 2014). The rapid mix and flocculation processes were simulated with the jar tester by having one minute of mixing at 300 rpm ( $G = 360 s^{-1}$ ) followed by two hours of mixing at 60 rpm ( $G = 54 s^{-1}$ ) (Phipps & Bird, 2021). The mean velocity gradient required for full scale rapid mix processes cannot be obtained using a jar tester, but the largest mean velocity gradient possible was used. The detention time for full scale rapid mix ranges from a few seconds to 1 minutes, while the detention time for full scale flocculation ranges from a few minutes to an hour (Metcalf & Eddy, 2014). The jar test experiments were operated for a similar time frame as full scale drinking water treatment processes.

Removal of PFHxS, PFOS, and PFOA by adsorbents concentrations ranging from 0 to 1000 mg/L are shown in Figure 4-1. PAC at a dose of 10 mg/L had complete adsorption of PFHxS and PFOS, while a PAC dose of 100 mg/L was required for complete adsorption of PFOA. The discussion of the PFAS removal by the biochar focuses on the results obtained with low (100 mg/L) and high (1000 mg/L) biochar concentrations.

Low doses of the biochars were not very effective at adsorbing any of the PFAS compounds. PFHxS, PFOA, and PFOS concentrations were reduced 13%, 1.7%, and 22%, respectively, by 100 mg/L of halophyte biochar BGNDRF. Bone char was the most effective biochar. At a dose of 100 mg/L of bone char, PFHxS and PFOS concentrations



were reduced 23%, but no reduction in the concentration of PFOA was observed. Halophyte biochar NMSU (100 mg/L) achieved the least reduction in PFAS (0% for PFHxS, -7.8% for PFOA, and 4.2% for PFOS.) Based on the results of the first jar test experiments, the biochar doses were increased to 200, 500 and 1000 mg/L in hopes of seeing improved adsorption.

At adsorbent concentrations of 1000 mg/L, halophyte biochar BGNDRF exhibited the best PFAS removal among the biochars. At this high concentration, it removed 100% of the PFHxS and PFOS and reduced PFOA 86%. Bone char reduced PFHxS, PFOS, and PFOA concentrations 62%, 100% and 38%, respectively. Halophyte biochar NMSU did not adsorb any PFHxS, whereas the PFOS and PFOA concentrations were reduced 64% and 7.7%, respectively.

Overall PFOA was the most difficult PFAS compound for all the adsorbents to remove likely because it occurred at a higher concentration in the groundwater. The weaker acidity of the carboxylic acid functional group in PFOA, in comparison to the sulfonic acid functional group in PFOS, could have contributed to the lower observed reductions in PFOA concentrations compared with PFOS (Zheng et al., 2021). PFOS was removed most effectively by all the adsorbents. Lower PFOA adsorption compared to PFOS is consistent with findings reported in other published studies (Deng et al., 2015, Kundu et al., 2021, Zheng et al., 2021).

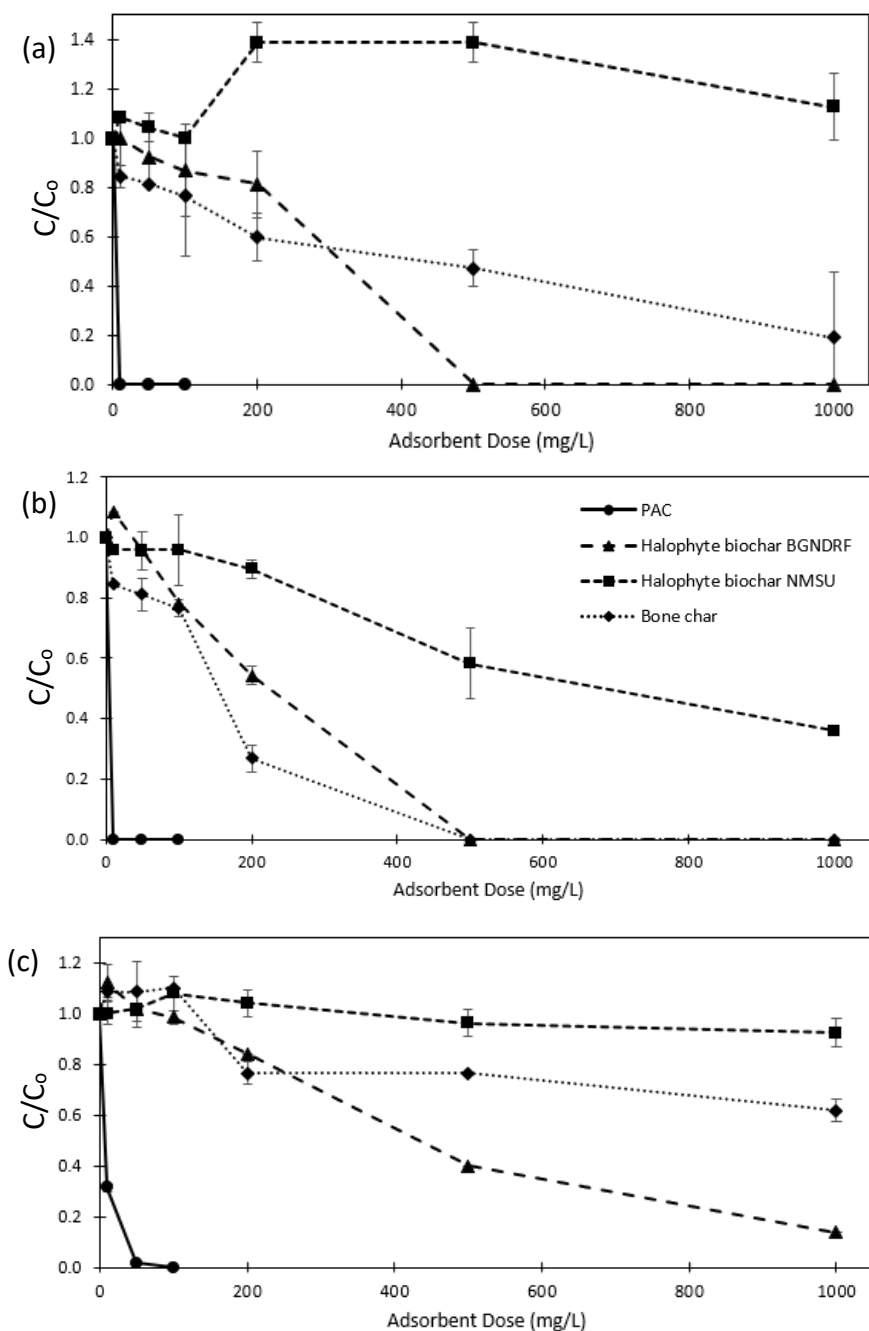


**Figure 4-1:** Normalized concentrations of (a) PFHxS, (b) PFOS, and (c) PFOA as a function of adsorbent doses from 0-1000 mg/L. Where C represents final concentration, and  $C_0$  represents the initial concentration. Error bars indicate  $\pm 1$  standard deviation of duplicate measurements.

The equilibrium parameters for PFOA, PFOS, and PFHxS were estimated for the halophyte biochar BGNDRF and shown in Figure 4-2. Based on the shape of the graphs, a Langmuir isotherm is the most appropriate fit. The graphs suggest that a maximum sorption capacity was reached at 285 ng/L, 18 ng/L and 12 ng/L for PFOA, PFOS, and PFHxS respectively. The maximum sorption capacity ( $q_{\max}$ ) was 0.00005 mg/g for PFOA and PFOS, and 0.00002 mg/g for PFHxS. The  $q_{\max}$  for PFOA and PFOS are significantly lower than reported in literature (Table 4-3). PFHxS is not as widely studied as PFOA and PFOS and there were no reported  $q_{\max}$  values in literature. The time to reach adsorption equilibrium varies widely ranging from a few hours for PAC to 16 days for some biochars (Du et al., 2014). It is likely that in this current study, the time frame of 2 hours was not sufficient to reach the sorption equilibrium.

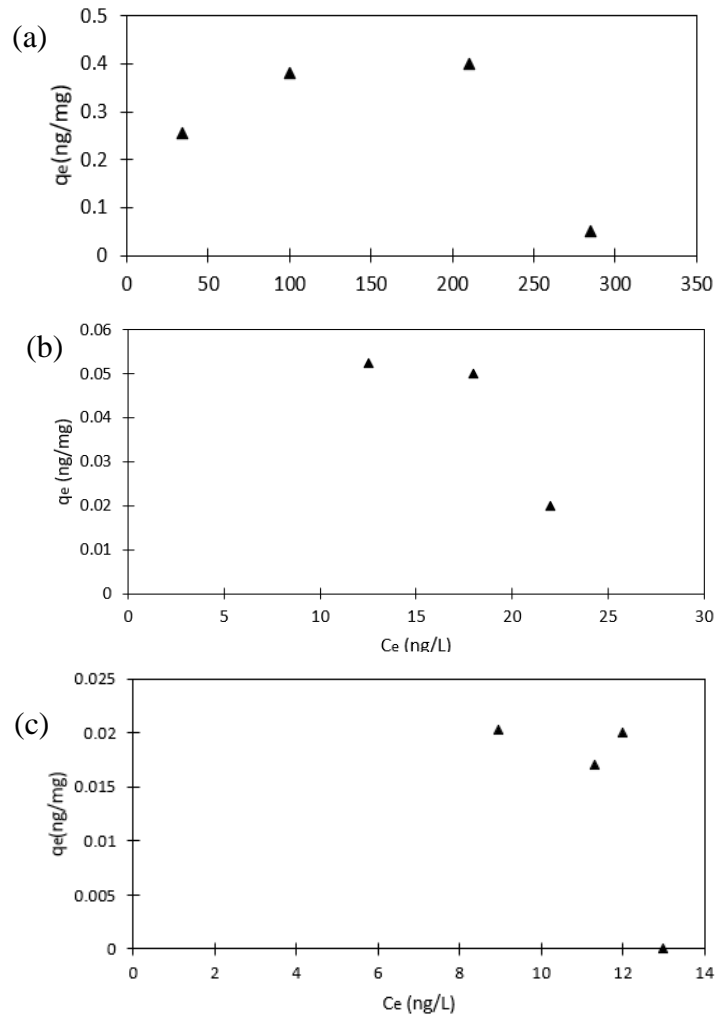


**Figure 4-2:** Concentration ( $C_e$ ) of (a) PFOA, (b) PFOS, and (c) PFHxS after two hours versus the adsorption capacity at equilibrium ( $q_e$ ) for halophyte biochar BGNDRF.

**Table 4-3:** Maximum sorption capacity of biochars and PAC for PFOA, PFOS, and PFHxS reported in adsorption studies

Adsorbent	PFAS	q <sub>max</sub> (mg/g)	Source
Softwood	PFOA	21.56	Zhang et al. (2021)
	PFOS	35.21	
Bamboo derived GAC	PFOA	476.18	Deng et al. (2015)
	PFOS	1160.3	
PAC	PFOA	15.73-434.77	
	PFOS	365.09-715.18	
Pinewood	PFOA	41.3	Inyang & Dickenson. (2017)
Hardwood	PFOA	41.2	
Halophyte biochar	PFOA	0.00005	This study
	PFOS	0.00005	
BGNDRF	PFHxS	0.00002	

### 4.3 Impacts of adsorbents on DOM and aqueous inorganic ions concentrations

The chemical and physical properties of the groundwater, including PFAS concentrations, were characterized following the methods described in Section 3-6. The results of these analyses are summarized in Table 4-4.

**Table 4-4:** Chemical and physical properties of untreated groundwater obtained from Well 2

Parameter	Value <sup>1</sup>	Units
pH	8.03 ± 0.11	
Alkalinity	239 ± 1.8	mg/L as CaCO <sub>3</sub>
Conductivity	6.16 ± 0.04	mS
Dissolved organic carbon (DOC) concentration	1.47 ± 0.38	mg/L
Temperature	24.7 ± 1.3	°C
A <sub>254</sub>	0.019 ± 0.002	cm <sup>-1</sup>
PFOA (C <sub>8</sub> HF <sub>15</sub> O <sub>2</sub> ) concentration	293 ± 29.1	ng/L
PFOS (C <sub>8</sub> HF <sub>17</sub> O <sub>3</sub> S) concentration	24.3 ± 3.4	ng/L
PFHxS (C <sub>6</sub> HF <sub>13</sub> O <sub>3</sub> S) concentration	12.9 ± 2.9	ng/L

<sup>1</sup>Average ± 1 standard deviation (n = 7)

The results of the jar test assays to quantify DOC adsorption by the biochars and PAC are shown in Figure 4-3. DOC removal increased with PAC concentration, and at a PAC concentration of 50 mg/L, complete removal of DOC was observed. DOC removal by the three biochars was much lower and was relatively constant (6 to 21%) at varying adsorbent concentrations. Interestingly, all biochars achieved optimal DOC removal at an adsorbent dose of 200 mg/L. At this adsorbent concentration, DOC removals were 60% for halophyte biochar BGNDRF, 32% for halophyte biochar NMSU, and 29% for bone char. At adsorbent doses greater than 200 mg/L, halophyte biochar NMSU and bone char exhibited final aqueous DOC concentrations that exceeded the initial DOC concentrations. It is hypothesized that the increase in concentration could be the result of DOC desorption or leaching of organics that were not removed during pyrolysis.

The  $A_{254}$  absorbance of aqueous samples treated with the biochars and PAC was analyzed to give a better indication of the type of dissolved organic matter (DOM) in the samples. DOM is large complex material that is predominantly carbon but also includes nitrogen, hydrogen, and oxygen, while DOC refers to the concentration of dissolved carbon. In general, the compounds quantified by measuring the absorbance at 254 nm are larger organic compounds with higher aromaticity and more adsorbable than bulk DOC. Therefore, it was expected that DOM would be adsorbed more effectively than DOC, unless the DOM compounds are too large to enter macropores (particle diameter > 50 nm) (Crittenden, 2012). The results of the jar test assays to quantify the reduction in  $A_{254}$  by the biochars and PAC are also shown in Figure 4-3. The reduction in  $A_{254}$  due to adsorption onto PAC increased from 45 to 71% as the PAC concentration increased. Compared with PAC, the three biochars achieved much lower reductions in the  $A_{254}$ . The reduction in  $A_{254}$  increased slightly (from 3 to 20%) for all three biochars with increasing adsorbent dose (up to 200 mg/L). At adsorbent doses greater than 200 mg/L, halophyte biochar BGNDRF achieved a consistent reduction in  $A_{254}$  of 27 to 32%, but concentrations of bone and halophyte NMSU biochars of >200 mg/L resulted in  $A_{254}$  absorbances that exceeded the  $A_{254}$  of untreated water. It is hypothesized that the increase in absorbance could be the result of DOM desorption or leaching of organics that were not removed during pyrolysis. None of the adsorbents were able to remove all the DOM in groundwater. There was not a desired treatment standard for DOM concentrations in the treated groundwater, but full scale treatment using biochar or PAC may require treatment standards for DOM.

Background DOM present in water has been shown to impact the adsorption affinity of PFAS to biochar and PAC by competing for adsorption sites, blocking pores, and causing electrostatic repulsion between the adsorbent and PFAS (Gagliano, 2020, Inyang & Dickenson, 2017, Steigerwald & Ray, 2021). Additionally, small concentrations of DOM can alter the surface charge of the adsorbent drastically either enhancing or limiting PFAS adsorption (Inyang & Dickenson, 2017). DOM in the groundwater in this study can be assessed by measuring the concentration of DOC. The DOC was low ( $1.5 \pm 0.4$  mg/L) but would still be expected to impact adsorption of PFAS significantly based on the results of other studies.

In addition, the solution pH can have significant impacts on adsorption affinity of PFAS because it can alter the charge of both adsorbents and DOM. Kundu et al. (2021), Zhang et al. (2021), and Deng et al. (2015) reported that decreasing pH increased adsorption of PFAS compounds onto biochars. When divalent ions ( $\text{Ca}^{2+}$  and  $\text{Mg}^{2+}$ ) are added to a solution containing PFAS, PFAS sorption to biochar may increase with increasing pH because of divalent cation bridging effects (Du et al., 2014). The divalent cation bridging effect involves the cations binding to the negatively charged surface functional groups on the adsorbent surface (carboxyl, phenolic, hydroxyl) which forms a bridge between the PFAS anions (Du et al., 2014). In the current study, the impacts of pH on PFAS adsorption were not investigated, but the pH used has significant impacts on adsorption capabilities. The pH was relatively constant ranging from 8.0 to 8.7 with the higher pH values occurring at high adsorbent doses (500 – 1000 mg/L). If the  $\text{pH}_{\text{zpc}}$  of the adsorbents was measured, the adsorbent's surface charge at the experimental pH would be known. The adsorbent's  $\text{pH}_{\text{zpc}}$  provides a better understanding of the dominant mechanism for adsorption of PFOA, PFOS, and PFHxS onto biochar and allows for the selection of the optimal pH for adsorption to be studied.

Another water quality parameter that can impact PFAS adsorption is the concentrations of inorganic ions in solutions. The impacts can include the compression of the electrical double layer and neutralization of the surface charge of the adsorbent, salting out, competitive adsorption, and divalent cation bridging effects (Zhang et al., 2019, Du et al., 2014). This is relevant to the current study because the untreated groundwater used in this study had a very high TDS concentration ( $5,322 \pm 625$  mg/L). Sulfate was present at the highest concentration ( $2,811 \pm 530$  mg/L). Sodium, chloride, calcium, and magnesium ions were also present in high concentrations. The high concentrations of inorganic ions may have resulted in any one of the above listed effects occurring, thereby enhancing PFAS adsorption by increasing the probability of interactions between PFAS and the adsorbent at the adsorbent's surface. Additional research is required to draw further conclusions about the impact of inorganic ions on adsorption of PFAS in solution.

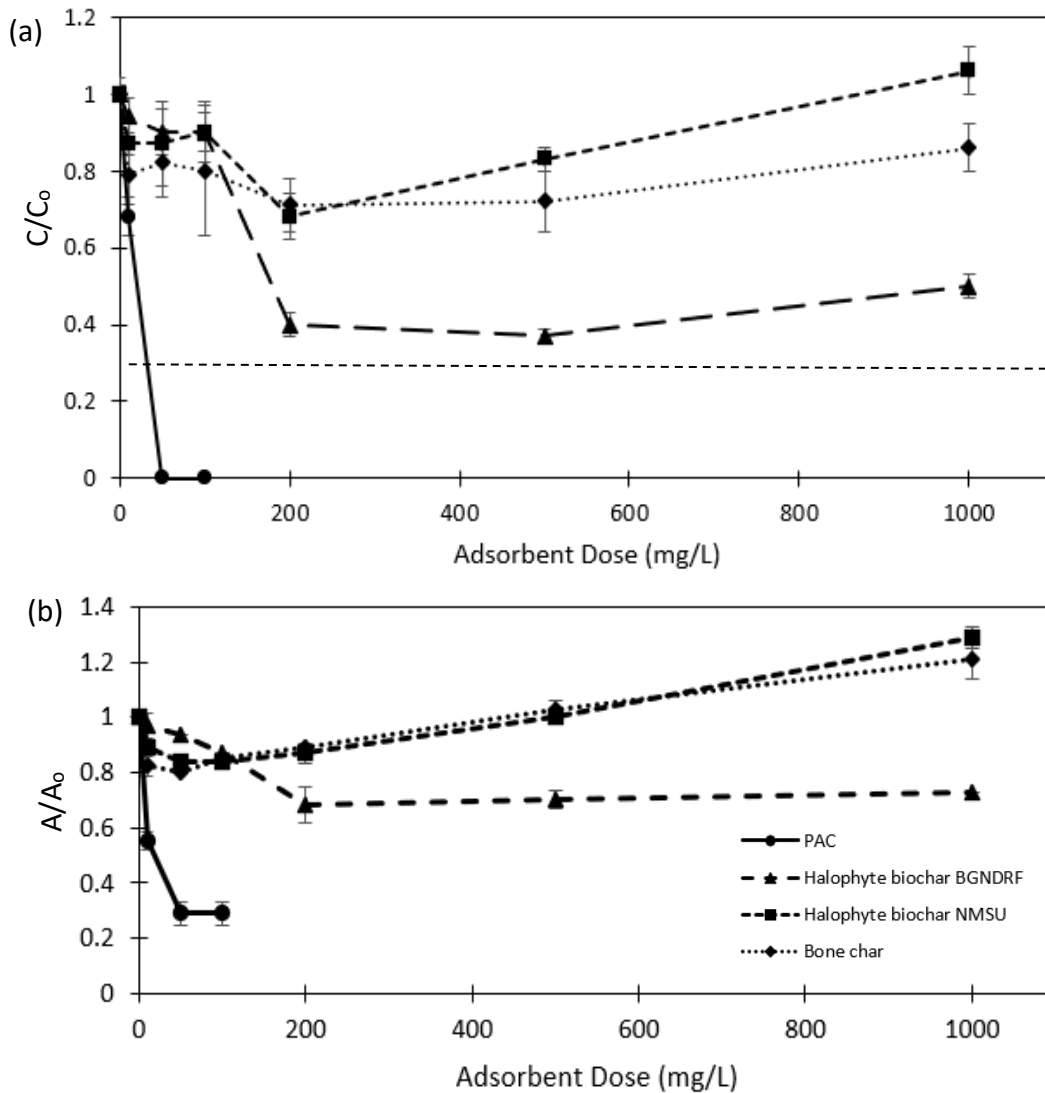


**Figure 4-3:** (a) Normalized DOC concentration and (b) normalized  $A_{254}$ , as a function of adsorbent dose. Error bars indicate standard deviation of duplicate jars, where  $C$  represents final concentration,  $C_0$  represents the initial concentration,  $A$  represents final absorbance, and  $A_0$  represents initial absorbance. Symbols represent the average of the replicate jars. Error bars represent  $\pm 1$  standard deviations of duplicate measurements. In panel (a), the dashed horizontal line represents the method detection limit (0.0616 mg/L).

The BGNDRF Well 2 groundwater contained high levels of nitrate, and the optimum wavelength for absorbance by nitrate (280 nm) is similar to that of DOM (254 nm). To ensure that the changes in the  $A_{254}$  values of the groundwater following treatment reflected adsorption of DOM, and not nitrate removal, the nitrate concentration in untreated Well 2 groundwater and in water treated with 100 mg/L of each adsorbent was

measured (Table 4-5). The nitrate concentrations in the treated waters were similar to the nitrate concentration in the untreated groundwater. This indicates that nitrate was not removed by any of the adsorbents, and, therefore, the reduction in  $A_{254}$  observed in treated water could be attributed to adsorption of DOC. Note that all the nitrate concentrations reported in Table 4-2 are considerably lower than the historical average nitrate concentration (7.2 mg/L) (BGNDRF, 2022). Most likely the low nitrate concentrations measured in the current study were caused by chloride interference. Chloride causes interference in the Hach nitrate assay at concentrations greater than 100 mg/L (Hach, 2014). Well 2 groundwater contains an average chloride concentration of 570 mg/L (BGNDRF, 2022). The chloride inference explains why the nitrate concentrations were significantly lower.

**Table 4-5:** Nitrate concentrations and  $A_{254}$  in untreated water and water treated with 100 mg/L of adsorbent.

Adsorbent Type	Nitrate ( $\text{NO}_3^-$ )	$A_{254}$	
	(mg N/L) <sup>a</sup>	( $\text{cm}^{-1}$ ) <sup>a</sup>	$C/C_0$ <sup>b,c</sup>
Untreated Water	$5.0 \pm 0.1$	$0.022 \pm 0.001$	1.0
PAC	$5.1 \pm 0.0$	$0.005 \pm 0.001$	0.21
Halophyte biochar BGNDRF	$4.9 \pm 0.1$	$0.015 \pm 0.000$	0.68
Halophyte biochar NMSU	$4.6 \pm 0.6$	$0.017 \pm 0.000$	0.77
Bone Char	$4.9 \pm 0.4$	$0.017 \pm 0.001$	0.77

a Average  $\pm$  standard deviation (n=2)

b Average (2 jars)

c  $C/C_0$  Normalized concentration



## 5 Summary and Future Work

PAC outperformed the halophytes and cow bone biochars at low adsorbent doses of 10 to 100 mg/L. The halophyte biochar BGNDRF had the best adsorption capabilities for PFAS of the three biochars tested. At a dose of 1000 mg/L, halophyte biochar BGNDRF was able to remove all PFOS and PFHxS present and remove 86% of PFOA. PAC had a surface area approximately 10 times greater than halophyte biochar BGNDRF and bone char and 100 times greater than halophyte biochar NMSU which explains the high adsorption capabilities of PAC. The higher pyrolysis temperature used to produce the halophyte biochar BGNDRF significantly increased its surface area compared with halophyte biochar NMSU.

Future work could focus on optimization of the pyrolysis temperature and technique for production of biochar using halophyte species *A. lentiformis*. For example, the addition of an activation process in biochar creation could significantly increase the surface area to be more comparable with PAC. Conducting the jar test experiments with different water sources (lake water, wastewater, and deionized water etc.) could be used to investigate the impacts of DOC and cation and anion concentrations on adsorption capabilities. It would also be informative to measure the  $\text{pH}_{\text{zpc}}$  of the biochars. Expanding the number of PFAS compounds in sorption studies will also be needed to fully evaluate the feasibility of using biochar adsorption to treat drinking water impacted by PFAS. Additionally, experiments estimating the equilibrium and kinetic sorption parameters of the biochars would allow the adsorption performance to be compared with other published biochar literature.

## 6 Reference List

Ahmad, M., Rajapaksha, A. U., Lim, J. E., Zhang, M., Bolan, N., Mohan, D., ... & Ok, Y. S. (2014). Biochar as a sorbent for contaminant management in soil and water: a review. *Chemosphere*, 99, 19-33.

Amidei, D. (2021). Carbon Adsorption Systems for Remediation of N-Nitrosodimethylamine (NDMA) From Groundwater. [Unpublished Doctoral Dissertation]. New Mexico State University.

American Public Health Association (APHA), American Water Works Association (AWWA), and Water Environment Association (WEA). (2017). Standard methods for the examination of water and wastewater. 23rd ed. Denver: AWWA.

American Water Works Association (AWWA). (2020). Drinking Water Treatment for PFAS Selection Guide.  
<https://www.awwa.org/Portals/0/AWWA/ETS/Resources/Technical%20Reports/Drinking-Water-Treatment-PFAS.pdf?ver=2020-11-10-100726-250>

Brackish Groundwater National Desalination Research Facility (BGNDRF). (February 20, 2022). Well Water Data. <https://www.usbr.gov/research/bgndrf/water.html>

Cantrell, K. B., Hunt, P. G., Uchimiya, M., Novak, J. M., & Ro, K. S. (2012). Impact of pyrolysis temperature and manure source on physicochemical characteristics of biochar. *Bioresource technology*, 107, 419-428.

Cerra, S., M.K. Shukla, and S. O'Meara. (2021). Determining Impacts of Long-Term Use of Reverse Osmosis Concentrate on Atriplex species, Soil Characteristics and Microbial Communities. Bureau of Reclamation, US Dept. of Interior. Final Report Number: ST-2021-1780-05.

Crittenden, J. C., R. R. Trussell, D. W. Hand, K. J. Howe, and G. Tchobanoglous. (2012). *MWH's water treatment: Principles and design*. Chapter 15.

3rd ed. Hoboken, NJ: Wiley.

Dai, Y., Zhang, N., Xing, C., Cui, Q., & Sun, Q. (2019). The adsorption, regeneration and engineering applications of biochar for removal organic pollutants: a review. *Chemosphere*, 223, 12-27.

Del Vento, S., Halsall, C., Gioia, R., Jones, K., & Dachs, J. (2012). Volatile per- and polyfluoroalkyl compounds in the remote atmosphere of the western Antarctic Peninsula: an indirect source of perfluoroalkyl acids to Antarctic waters?. *Atmospheric Pollution Research*, 3(4), 450-455

- Deng, S., Nie, Y., Du, Z., Huang, Q., Meng, P., Wang, B., ... & Yu, G. (2015). Enhanced adsorption of perfluorooctane sulfonate and perfluorooctanoate by bamboo-derived granular activated carbon. *Journal of hazardous materials*, 282, 150-157.
- Du, Z., Deng, S., Bei, Y., Huang, Q., Wang, B., Huang, J., & Yu, G. (2014). Adsorption behavior and mechanism of perfluorinated compounds on various adsorbents—A review. *Journal of hazardous materials*, 274, 443-454.
- U.S. Environmental Protection Agency (USEPA). (2020). Drinking Water Health Advisories for PFOA and PFOS. <https://www.epa.gov/ground-water-and-drinking-water/drinking-water-health-advisories-pfoa-and-pfos>
- Fenton, S. E., Ducatman, A., Boobis, A., DeWitt, J. C., Lau, C., Ng, C., ... & Roberts, S. M. (2021). Per-and polyfluoroalkyl substance toxicity and human health review: Current state of knowledge and strategies for informing future research. *Environmental toxicology and chemistry*, 40(3), 606-630.
- Fidel, R. B., Laird, D. A., Thompson, M. L., & Lawrinenko, M. (2017). Characterization and quantification of biochar alkalinity. *Chemosphere*, 167, 367-373.
- Gagliano, E., Sgroi, M., Falciglia, P. P., Vagliasindi, F. G., & Roccaro, P. (2020). Removal of poly-and perfluoroalkyl substances (PFAS) from water by adsorption: Role of PFAS chain length, effect of organic matter and challenges in adsorbent regeneration. *Water research*, 171, 115381.
- Guo, W., Huo, S., Feng, J., & Lu, X. (2017). Adsorption of perfluorooctane sulfonate (PFOS) on corn straw-derived biochar prepared at different pyrolytic temperatures. *Journal of the Taiwan Institute of Chemical Engineers*, 78, 265-271.
- Hach. (2014). Nitrate, MR Cadmium Reduction Method 8171, Powder Pillows or AccuVac Ampuls. <https://www.hach.com/nitraver-5-nitrate-reagent-powder-pillows-10-ml-pk-100/product-downloads?id=7640208933&callback=qs>
- Hopkins, Z. R., Sun, M., DeWitt, J. C., & Knappe, D. R. (2018). Recently detected drinking water contaminants: GenX and other per-and polyfluoroalkyl ether acids. *Journal-American Water Works Association*, 110(7), 13-28.
- Inyang, M., & Dickenson, E. R. (2017). The use of carbon adsorbents for the removal of perfluoroalkyl acids from potable reuse systems. *Chemosphere*, 184, 168-175.
- Kundu, S., Patel, S., Halder, P., Patel, T., Marzbali, M. H., Pramanik, B. K., ... & Shah, K. (2021). Removal of PFASs from biosolids using a semi-pilot scale pyrolysis reactor and the application of biosolids derived biochar for the removal of PFASs from contaminated water. *Environmental Science: Water Research & Technology*, 7(3), 638-649.

- Kennedy, A. M., & Arias-Paic, M. (2020). Fixed-bed adsorption comparisons of bone char and activated alumina for the removal of fluoride from drinking water. *Journal of Environmental Engineering*, 146(1), 04019099.
- Li, Q., Snoeyink, V. L., Mariñas, B. J., & Campos, C. (2003). Pore blockage effect of NOM on atrazine adsorption kinetics of PAC: the roles of PAC pore size distribution and NOM molecular weight. *Water research*, 37(20), 4863-4872.
- Malcolm Pirnie, Inc. (November, 2003). Water Well Construction Log and Drilling Diagram.
- Metcalf & Eddy. (2014). Wastewater Engineering: Treatment and Resource Recovery. (5<sup>th</sup> ed.). McGraw Hill.
- New Mexico Environment Department (NMED). (2021) PFAS Data. <https://www.env.nm.gov/pfas/data/>
- New Mexico Environment Department (NMED). (2019). PFAS Water Testing Results. <https://www.env.nm.gov/wp-content/uploads/sites/21/2019/04/Alamogordo-Holloman-PFAS-sample-results.pdf>
- Newton, B. Talon & Land, Lewis (2016). Brackish Water Assessment in the Eastern Tularosa Basin, New Mexico. New Mexico Bureau of Geology and Mineral Resources. [https://geoinfo.nmt.edu/publications/openfile/downloads/500-599/582/OFR-582\\_ETB\\_brackishLR.pdf](https://geoinfo.nmt.edu/publications/openfile/downloads/500-599/582/OFR-582_ETB_brackishLR.pdf)
- Organization for Economic Co-operation and Development. (OECD). (2018). Toward a new comprehensive global database of per- and polyfluoroalkyl substances (PFASs): summary report on updating the OECD 2007 List of per- and polyfluoroalkyl substances (PFASs). Contract No.: JT03431231.
- Phipps & Bird. (2021). A Simplified Jar Test Procedure.
- Pontius, F. (2019). Regulation of perfluorooctanoic acid (PFOA) and perfluorooctane sulfonic acid (PFOS) in drinking water: A comprehensive review. *Water*, 11(10), 2003.
- Steigerwald, J. M., & Ray, J. R. (2021). Adsorption behavior of perfluorooctanesulfonate (PFOS) onto activated spent coffee grounds biochar in synthetic wastewater effluent. *Journal of Hazardous Materials Letters*, 2, 100025.
- Sun, M., Arevalo, E., Strynar, M., Lindstrom, A., Richardson, M., Kearns, B., Knappe, D. R. (2016) Legacy and emerging perfluoroalkyl substances are important drinking water contaminants in the Cape Fear River Watershed of North Carolina. *Environmental Sci. & Technol. Letters*, 3(12), 415-419.
- Tan, X., Liu, Y., Zeng, G., Wang, X., Hu, X., Gu, Y., & Yang, Z. (2015). Application of biochar for the removal of pollutants from aqueous solutions. *Chemosphere*, 125, 70-85.

Teaf, C. M., Garber, M. M., Covert, D. J., & Tuovila, B. J. (2019). Perfluorooctanoic acid (PFOA): environmental sources, chemistry, toxicology, and potential risks. *Soil and Sediment Contamination: An International Journal*, 28(3), 258-273.

Wanninayake, D. M. (2021). Comparison of currently available PFAS remediation technologies in water: A review. *Journal of Environmental Management*, 283, 111977.

Wei, J., Tu, C., Yuan, G., Liu, Y., Bi, D., Xiao, L., ... & Zhang, X. (2019). Assessing the effect of pyrolysis temperature on the molecular properties and copper sorption capacity of a halophyte biochar. *Environmental Pollution*, 251, 56-65.

XTech Lab Supplies. (2022). Crucibles and Labware.  
<https://www.xtechlabsupplies.com/crucibles-and-labware.html>

Zhang, Y., Idowu, O. J., & Brewer, C. E. (2016). Using agricultural residue biochar to improve soil quality of desert soils. *Agriculture*, 6(1), 10.

Zhang, D. Q., Zhang, W. L., & Liang, Y. N. (2019). Adsorption of perfluoroalkyl and polyfluoroalkyl substances (PFASs) from aqueous solution-A review. *Science of The Total Environment*, 694, 133606.

Zhang, D., He, Q., Wang, M., Zhang, W., & Liang, Y. (2021). Sorption of perfluoroalkylated substances (PFASs) onto granular activated carbon and biochar. *Environmental technology*, 42(12), 1798-1809.

## A Appendix

Table A-1: PAC jar test alkalinity, pH, temperature,  $A_{254}$ , and conductivity for doses of 10, 50 and 100 mg/L

Jar Number	Dose (mg/L)	Alkalinity (mg/L as $\text{CaCO}_3$ )	pH (su)	Temperature ( $^{\circ}\text{C}$ )	$\text{UVA}_{254}$ ( $\text{cm}^{-1}$ )	C/ $C_0$	Conductivity (mS)
raw	0	240	8.23	25.6	0.019	1.00	6.22
1	10	--	8.33	25.4	0.010	0.53	6.26
2	50	--	8.35	24.5	0.005	0.26	6.25
3	100	--	8.38	24.6	0.006	0.32	6.25
4	10	--	8.36	24.6	0.011	0.58	6.27
5	50	--	8.38	24.7	0.006	0.32	6.25
6	100	--	8.35	24.6	0.005	0.26	6.25

Table A-2: Halophyte (BGNDRF) jar test alkalinity, pH, temperature, A<sub>254</sub>, and conductivity for doses of 10, 50 and 100 mg/L

Jar Number	Dose (mg/L)	Alkalinity (mg/L as CaCO <sub>3</sub> )	pH (su)	Temperature (°C)	UVA <sub>254</sub>		Conductivity (mS)
					(cm <sup>-1</sup> )	C/C <sub>0</sub>	
raw	0	240	7.96	26.6	0.016	1.00	6.14
1	10	--	8.07	24.7	0.016	1.00	6.23
2	50	--	8.16	24.6	0.015	0.94	6.23
3	100	--	8.22	24.5	0.014	0.88	6.23
4	10	--	8.06	24.6	0.015	0.94	6.23
5	50	--	8.16	24.6	0.015	0.94	6.24
6	100	--	8.18	24.7	0.014	0.88	6.22

Table A-3: Halophyte (NMSU) jar test alkalinity, pH, temperature, A<sub>254</sub>, and conductivity for doses of 10, 50 and 100 mg/L

Jar Number	Dose (mg/L)	Alkalinity (mg/L as CaCO <sub>3</sub> )	pH (su)	Temperature (°C)	UVA <sub>254</sub>		Conductivity (mS)
					(cm <sup>-1</sup> )	C/C <sub>0</sub>	
raw	0	238	8.03	25.4	0.019	1.00	6.11
1	10	--	8.08	24.1	0.017	0.89	6.21
2	50	--	8.12	24.0	0.016	0.84	6.22
3	100	--	8.22	24.1	0.016	0.84	6.23
4	10	--	8.08	24.3	0.017	0.89	6.23
5	50	--	8.10	24.3	0.016	0.84	6.24
6	100	--	8.22	24.4	0.016	0.84	6.23

Table A-4: Bone char jar test alkalinity, pH, temperature, A<sub>254</sub>, and conductivity for doses of 10, 50 and 100 mg/L

Jar Number	Dose (mg/L)	Alkalinity (mg/L as CaCO <sub>3</sub> )	pH (su)	Temperature (°C)	UVA <sub>254</sub>		Conductivity (mS)
					(cm <sup>-1</sup> )	C/C <sub>0</sub>	
raw	0	238	7.93	25	0.020	1.00	6.21
1	10	--	8.11	23	0.016	0.80	6.23
2	50	--	8.13	23	0.016	0.80	6.22
3	100	--	8.17	23	0.017	0.85	6.20
4	10	--	8.12	23	0.017	0.85	6.23
5	50	--	8.13	23	0.016	0.80	6.22
6	100	--	8.15	23	0.017	0.85	6.22



Table A-5: Halophyte (BGNDRF) jar test alkalinity, pH, temperature, A<sub>254</sub>, and conductivity for doses of 200, 500 and 1000 mg/L

Jar Number	Dose (mg/L)	Alkalinity (mg/L as CaCO <sub>3</sub> )	pH (su)	Temperature (°C)	UVA <sub>254</sub>		Conductivity (mS)
					(cm <sup>-1</sup> )	C/C <sub>0</sub>	
raw	0	239	8.12	22	0.022	1.00	6.16
1	200	--	8.37	23	0.016	0.73	6.09
2	500	--	8.48	23	0.016	0.73	6.01
3	1000	--	8.66	23	0.016	0.73	5.92
4	200	--	8.42	23	0.014	0.64	6.05
5	500	--	8.53	23	0.015	0.68	6.01
6	1000	--	8.66	23	0.016	0.73	5.94

Table A-6: Halophyte (NMSU) jar test alkalinity, pH, temperature, A<sub>254</sub>, and conductivity for dose of 200, 500 and 1000 mg/L

Jar Number	Dose (mg/L)	Alkalinity (mg/L as CaCO <sub>3</sub> )	pH (su)	Temperature (°C)	UVA <sub>254</sub>		Conductivity (mS)
					(cm <sup>-1</sup> )	C/C <sub>0</sub>	
raw	0	243	7.96	24.2	0.019	1.00	6.15
1	200	--	8.35	22.8	0.016	0.84	6.09
2	500	--	8.47	22.8	0.019	1.00	6.04
3	1000	--	8.60	23.0	0.025	1.32	5.92
4	200	--	8.41	23.0	0.017	0.89	6.06
5	500	--	8.49	23.0	0.019	1.00	6.02
6	1000	--	8.62	23.1	0.024	1.26	5.96

Table A-7: Bone char jar test alkalinity, pH, temperature, A<sub>254</sub>, and conductivity for doses of 200, 500 and 1000 mg/L

Jar Number	Dose (mg/L)	Alkalinity (mg/L as CaCO <sub>3</sub> )	pH (su)	Temperature (°C)	UVA <sub>254</sub> (cm <sup>-1</sup> )	C/C <sub>0</sub>	Conductivity (mS)
raw	0	238	7.98	24.6	0.019	1.00	6.10
1	200	--	8.32	23.0	0.017	0.89	6.07
2	500	--	8.29	23.0	0.019	1.00	6.00
3	1000	--	8.21	23.3	0.022	1.16	5.88
4	200	--	8.30	23.2	0.017	0.89	6.07
5	500	--	8.30	23.4	0.020	1.05	5.98
6	1000	--	8.22	23.4	0.024	1.26	5.89

Table A-8: Nitrate absorbance for PAC, Halophyte (BGNDRF) and Halophyte (NMSU) biochar

Jar Number	Water Volume (L)	Dose (mg/L)	Adsorbent	pH (su)	Temperature (°C)	UVA <sub>254</sub> cm <sup>-1</sup>	C/C <sub>0</sub>	Nitrate (NO <sub>3</sub> <sup>-</sup> ) (mg/L)
raw	--	0		7.86	24	0.021	1.00	4.9
1	2.0	100	PAC	8.26	23	0.005	0.24	5.1
2	2.0	100	PAC	8.27	22	0.004	0.19	5.1
3	2.0	100	Halophyte (BGNDRF)	8.27	23	0.015	0.71	4.8
4	2.0	100	Halophyte (BGNDRF)	8.27	22	0.015	0.71	5
5	2.0	100	Halophyte (NMSU)	8.27	23	0.017	0.81	5
6	2.0	100	Halophyte (NMSU)	8.27	23	0.017	0.81	4.1

Table A-9: Nitrate absorbance for bone char

Jar Number	Water Volume (L)	Dose (mg/L)	Absorbent	pH (su)	Temperature (°C)	UVA <sub>254</sub>		Nitrate (NO <sub>3</sub> <sup>-</sup> ) (mg/L)
						cm <sup>-1</sup>	C/C <sub>0</sub>	
raw	--	0		7.95	24	0.023	1.00	5
1	2.0	100	Cow Bone	8.12	23	0.018	0.78	4.6
2	2.0	100	Cow Bone	8.15	23	0.016	0.70	5.1

Table A-10: DOC concentrations, average, standard deviation, normalized concentration, and removal for adsorbent doses 10, 50 and 100 mg/L

Adsorbent	Adsorbent Dose (mg/L)	DOC (mg/L)				Avg. DOC (mg/L)	St. Dev.	Normalized Concentration (C/C <sub>0</sub> )	Removal (%)
PAC	0	1.27	1.24	-	-	1.26	0.02	1.00	0
	10	0.908	0.897	0.824	0.797	0.86	0.05	0.68	32
	50	0.536	ND	ND	ND	0.00	0.00	0.00	100
	100	ND	ND	ND	ND	0.00	0.00	0.00	100
Halophyte (BGNDRF)	0	1.02	0.998	-	-	1.01	0.02	1.00	0
	10	1.01	0.945	0.943	0.892	0.95	0.05	0.94	6
	50	0.989	0.882	0.906	0.853	0.91	0.06	0.90	10
	100	0.967	0.94	0.861	0.867	0.91	0.05	0.90	10
Halophyte (NMSU)	0	1.15	1.1	-	-	1.13	0.04	1.00	0
	10	1.03	0.983	0.966	0.951	0.98	0.03	0.87	13
	50	1.06	1.06	0.952	0.836	0.98	0.11	0.87	13
	100	1.08	1.06	0.991	0.913	1.01	0.08	0.90	10
Bone Char	0	1.34	1.33	-	-	1.34	0.01	1.00	0
	10	0.993	1.17	1.04	1.04	1.06	0.08	0.79	21
	50	1.07	1.24	1.05	1.04	1.10	0.09	0.82	18
	100	1.2	0.824	1.15	1.12	1.07	0.17	0.80	20

Table A-11: DOC concentrations, average, standard deviation, normalized concentration, and removal for adsorbent doses 200, 500 and 1000 mg/L

Adsorbent	Adsorbent Dose (mg/L)	DOC (mg/L)				Avg. DOC (mg/L)	St. Dev.	Normalized Concentration (C/C <sub>0</sub> )	Removal (%)
Halophyte (BGNDRF)	0	1.94	2.02	-	-	1.98	0.06	1.00	0
	200	1.06	1.06	1.01	-	0.78	0.03	0.40	60
	500	0.992	0.952	0.988	-	0.73	0.02	0.37	63
	1000	0.995	1.02	0.941	0.967	0.98	0.03	0.50	50
Halophyte (NMSU)	0	1.85	1.99	-	-	1.92	0.10	1.00	0
	200	1.38	1.35	1.28	1.24	1.31	0.06	0.68	32
	500	1.57	1.61	1.57	1.62	1.59	0.03	0.83	17
	1000	1.97	2.05	2.03	2.12	2.04	0.06	1.06	-6
Bone	0	1.65	1.72	-	-	1.69	0.05	1.00	0
	200	1.27	1.21	1.17	1.11	1.19	0.07	0.71	29
	500	1.28	1.29	1.18	1.12	1.22	0.08	0.72	28
	1000	1.43	1.55	1.43	1.42	1.46	0.06	0.86	14

Table A-12: PFAS average concentrations, normalized concentrations and removal for doses of 10, 50 and 100 mg/L

Adsorbent	Adsorbent Dose (mg/L)	Avg. Concentration (ng/L)			Normalized Concentration (C/C <sub>0</sub> )			Removal (%)		
		PFHxS	PFOS	PFOA	PFHxS	PFOS	PFOA	PFHxS	PFOS	PFOA
PAC	0	11	19	290	1.00	1.00	1.00	0.00	0.00	0.00
	10	ND	ND	90.5	0.00	0.00	0.31	100.00	100.00	68.79
	50	ND	ND	4.45	0.00	0.00	0.02	100.00	100.00	98.47
	100	ND	ND	ND	0.00	0.00	0.00	100.00	100.00	100.00
Halophyte (BGNDRF)	0	13	23	290	1.00	1.00	1.00	0.00	0.00	0.00
	10	13	25	325	1.00	1.09	1.12	0.00	-8.70	-12.07
	50	12	22	295	0.92	0.96	1.02	7.69	4.35	-1.72
	100	11.3	18	285	0.87	0.78	0.98	13.08	21.74	1.72
Halophyte (NMSU)	0	12	24	320	1.00	1.00	1.00	0.00	0.00	0.00
	10	13	23	320	1.08	0.96	1.00	-8.33	4.17	0.00
	50	12.5	23	325	1.04	0.96	1.02	-4.17	4.17	-1.56
	100	12	23	345	1.00	0.96	1.08	0.00	4.17	-7.81
Bone Char	0	16	26	300	1.00	1.00	1.00	0.00	0.00	0.00
	10	13.5	25	325	0.84	0.84	1.08	15.63	15.63	-8.33
	50	13	22	325	0.81	0.81	1.08	18.75	18.75	-8.33
	100	12.25	18.5	330	0.77	0.77	1.10	23.44	23.44	-10.00

Table A-13: PFAS average concentrations, normalized concentrations and removal for doses of 200, 500 and 1000 mg/L

Adsorbent	Adsorbent Dose (mg/L)	Avg. Concentration (ng/L)			Normalized Concentration (C/C <sub>0</sub> )			Removal (%)		
		PFHxS	PFOS	PFOA	PFHxS	PFOS	PFOA	PFHxS	PFOS	PFOA
Halophyte (BGNDRF)	0	11	23	250	1.00	1.00	1.00	0.00	0.00	0.00
	200	8.95	12.5	210	0.81	0.54	0.84	18.64	45.65	16.00
	500	0	0	100	0.00	0.00	0.40	100.00	100.00	60.00
	1000	0	0	34	0.00	0.00	0.14	100.00	100.00	86.40
Halophyte (NMSU)	0	9	24	260	1.00	1.00	1.00	0.00	0.00	0.00
	200	12.5	21.5	270	1.39	0.90	1.04	-38.89	10.42	-3.85
	500	12.5	14	250	1.39	0.58	0.96	-38.89	41.67	3.85
	1000	10.15	8.65	240	1.13	0.36	0.92	-12.78	63.96	7.69
Bone Char	0	18	31	340	1.00	1.00	1.00	0.00	0.00	0.00
	200	10.75	8.3	260	0.60	0.60	0.76	40.28	73.23	23.53
	500	8.45	0	260	0.47	0.47	0.76	53.06	100.00	23.53
	1000	6.8	0	210	0.38	0.38	0.62	62.22	100.00	38.24

Table A-14: PFAS concentration data, average concentration, and standard deviations for doses 10, 50 and 100 mg/L

Adsorbent	Dose (mg/L)	PFHxS				PFOS				PFOA			
		Conc. (ng/L)	Avg. Conc. (ng/L)	St. Dev.		Conc. (ng/L)	Avg. Conc. (ng/L)	St. Dev.		Conc. (ng/L)	Avg. Conc. (ng/L)	St. Dev.	
PAC	0	11	-	11	0.00	19	-	19	0.00	290		290	0.00
	10	0	0	0	0.00	0	0	0	0.00	94	87	90.5	0.02
	50	0	0	0	0.00	0	0	0	0.00	4.5	4.4	4.45	0.01
	100	0	0	0	0.00	0	0	0	0.00	0	0	0	0.00
Halophyte (BGNDRF)	0	13	-	13	0.00	23	-	0	0.00	290	-	290	0.00
	10	12	14	13	0.11	25	25	25	0.00	310	340	325	0.07
	50	11	13	12	0.11	21	23	22	0.06	280	310	295	0.07
	100	13	9.6	11.3	0.18	18	18	18	0.00	280	290	285	0.02
Halophyte (NMSU)	0	12	-	12	0.00	24	-	24	0.00	320	-	320	0.00
	10	13	13	13	0.00	23	23	23	0.00	310	330	320	0.04
	50	13	12	12.5	0.06	23	23	23	0.00	320	330	325	0.02
	100	12	12	12	0.00	25	21	23	0.12	330	360	345	0.07
Bone Char	0	16	-	0	0.00	26	-	0	0.00	300	-	300	0.00
	10	13	14	13.5	0.04	25	25	25	0.00	320	330	325	0.02
	50	13	13	13	0.00	21	23	22	0.05	300	350	325	0.12
	100	15	9.5	12.25	0.24	18	19	18.5	0.03	330	330	330	0.00



Table A-15: PFAS concentration data, average concentration, and standard deviations for doses 200, 500 and 1000 mg/L

Adsorbent	Dose (mg/L)	PFHxS				PFOS				PFOA			
		Conc. (ng/L)	Avg. Conc. (ng/L)	St. Dev.	Conc. (ng/L)	Conc. (ng/L)	Avg. Conc. (ng/L)	St. Dev.	Conc. (ng/L)	Conc. (ng/L)	Avg. Conc. (ng/L)	St. Dev.	
Halophyte (BGNDRF)	0	11	-	11	0.00	23	-	23	0.00	250	-	0	0.00
	200	10	7.9	8.95	0.13	13	12	12.5	0.03	210	210	210	0.00
	500	0	0	0	0.00	0	0	0	0.00	100	100	100	0.00
	1000	0	0	0	0.00	0	0	0	0.00	34	34	34	0.00
Halophyte (NMSU)	0	9	-	9	0.00	24	-	24	0.00	260	-	260	0.00
	200	12	13	12.5	0.08	21	22	21.5	0.03	260	280	270	0.05
	500	12	13	12.5	0.08	12	16	14	0.12	240	260	250	0.05
	1000	9.3	11	10.15	0.13	8.5	8.8	8.65	0.01	230	250	240	0.05
Bone Char	0	18	-	18	0.00	31	-	31	0.00	340	-	340	0.00
	200	9.5	12	10.75	0.10	7.3	9.3	8.3	0.05	250	270	260	0.04
	500	7.5	9.4	8.45	0.07	0	0	0	0.00	260	260	260	0.00
	1000	6.8	0	3.4	0.27	0	0	0	0.00	220	200	210	0.04

Table A-16: PFOA, PFOS, and PFHxS adsorption capacity at equilibrium

Adsorbent	PFOA		PFOS		PFHxS	
Dose (mg/L)	C <sub>e</sub> (ng/L)	q <sub>e</sub> (ng/mg)	C <sub>e</sub> (ng/L)	q <sub>e</sub> (ng/mg)	C <sub>e</sub> (ng/L)	q <sub>e</sub> (ng/mg)
0	290	-	23	-	13	-
10	325	-	25	-	13	0
50	295	-	22	0.02	12	0.02
100	285	0.05	18	0.05	11.3	0.017
200	210	0.40	12.5	0.05	8.95	0.020
500	100	0.38	0	-	0	-
1000	34	0.25	0	-	0	-